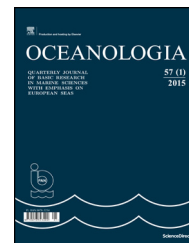




Available online at www.sciencedirect.com

ScienceDirect

journal homepage: www.elsevier.com/locate/oceano



ORIGINAL RESEARCH ARTICLE

Characteristics of the spring/summer production in the Mecklenburg Bight (Baltic Sea) as revealed by long-term pCO₂ data

B. Schneider^{a,*}, S. Buecker^a, S. Kaitala^b, P. Maunula^b, N. Wasmund^a

^a Leibniz Institute for Baltic Sea Research (IOW), Warnemünde, Germany

^b Finnish Environment Institute (SYKE), Helsinki, Finland

Received 18 March 2015; accepted 8 July 2015

Available online 22 July 2015

KEYWORDS

Mecklenburg Bight;
CO₂ partial pressure;
Spring bloom;
Nitrogen fixation

Summary Automated CO₂ partial pressure, pCO₂, measurements were performed on a cargo ship that commutes between the Gulf of Finland and the Mecklenburg Bight in the southwest of the Baltic Sea. The data from 2004 to 2014 along a sub-transect in the Mecklenburg Bight are used to analyze the timing and intensity of the net community production (NCP). The start of the spring bloom, identified by the first continuous drop of the pCO₂ below the atmospheric level, spanned from mid-February to mid-March. Converting the pCO₂ decrease during spring to changes in the total CO₂ concentration and taking into account air-sea gas exchange, the spring NCP was determined. The NCP increased by about 80% during 2004–2014, the mean amounted to 40 μmol L⁻¹. In two years a distinct second pCO₂ minimum in mid-summer succeeded the minimum in spring. This was attributed to production fuelled by nitrogen fixation since the nitrate concentrations were virtually zero and since the atmospheric deposition could not satisfy the NCP nitrogen demand. Furthermore, investigations of the plankton composition revealed a cyanobacteria biomass peak in the year with the highest mid-summer NCP. Based on the calculation of the mid-summer NCP in the two particular years and on the C/N ratio of particulate organic matter, the corresponding nitrogen fixation activity was calculated. These values and the analysis of the relationship between the integrated NCP and temperature indicated that the

* Corresponding author at: Leibniz Institute for Baltic Sea Research (IOW), 18119 Warnemünde, Germany. Tel.: +49 3815197320.

E-mail address: bernd.schneider@io-warnemuende.de (B. Schneider).

Peer review under the responsibility of Institute of Oceanology of the Polish Academy of Sciences.



Production and hosting by Elsevier

<http://dx.doi.org/10.1016/j.oceano.2015.07.001>

0078-3234/© 2015 Institute of Oceanology of the Polish Academy of Sciences. Production and hosting by Elsevier Sp. z o.o. This is an open access article under the CC BY-NC-ND license (<http://creativecommons.org/licenses/by-nc-nd/4.0/>).

nitrogen fixation activity in the Mecklenburg Bight was by a factor 3–4 lower than in the central Baltic Sea.

© 2015 Institute of Oceanology of the Polish Academy of Sciences. Production and hosting by Elsevier Sp. z o.o. This is an open access article under the CC BY-NC-ND license (<http://creativecommons.org/licenses/by-nc-nd/4.0/>).

1. Introduction

A fully automated measurement system for the continuous recording of the surface water CO_2 partial pressure, pCO_2 , was deployed on cargo ship “Finnpartner” in summer 2003. The ship commuted regularly at 2–3 days intervals between the Gulf of Finland in the northeast and the Mecklenburg Bight in the southwest of the Baltic Proper (Fig. 1). In 2007 the instrumentation was moved to cargo ship “Finnmaid” that had taken over the line of “Finnpartner”, and since then the measurements are continued. Because biochemical processes such as biomass (organic matter) production and mineralization (respiration) are intimately connected with the consumption and generation of CO_2 , respectively, the high resolution of the pCO_2 data can be used to detect and quantify plankton bloom events and their relationship to the availability of nitrogen and phosphorus in the various regions of the Baltic Proper. This approach is similar to the use of oxygen concentrations as an indicator for biomass production (e.g. Stigebrandt, 1991). However, since O_2 equilibrates relatively fast with the atmosphere,

the O_2 gas exchange constitutes a major term in the O_2 budget calculation and increases the uncertainty of the production estimate. In contrast, equilibration of CO_2 with the atmosphere is 5–10 times slower and the biologically induced changes of the CO_2 budget are conserved for a longer time in the water column and are less affected by CO_2 gas exchange.

Previous analysis of the pCO_2 data were mainly confined to the Baltic Proper and in particular to the eastern Gotland Sea (Schneider et al., 2014b; Schneider et al., 2006; Schneider et al., 2009). A characteristic bimodal seasonal distribution pattern with minima in May and in July was observed. These were attributed to the spring bloom and to the mid-summer production period fuelled by nitrogen fixation. Based on a CO_2 mass balance that included the gas exchange with the atmosphere, the net community production (NCP) during spring (April/May) was estimated and it was shown that the net production after the nitrate depletion by mid-April requires an external nitrogen source. However, the hypothesis of a spring nitrogen fixation (termed “cold fixation”) could not yet be confirmed by other methods.

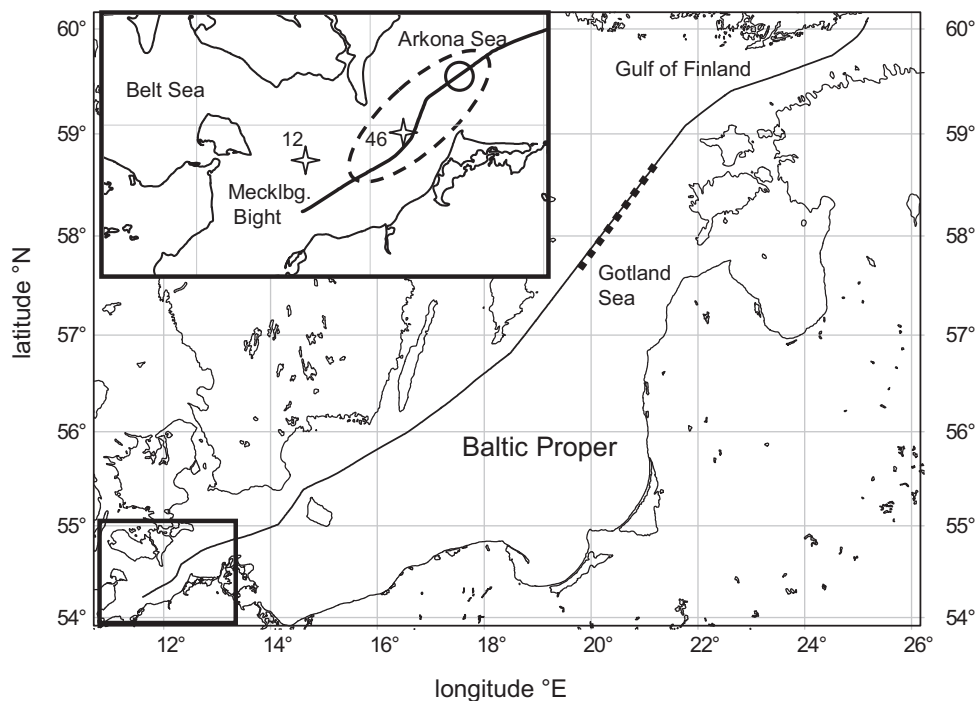


Figure 1 Route of the cargo ship “Finnmaid” (“Finnpartner”) between the Gulf of Finland and the southwest Baltic Sea. The dotted sub-transect in the Gotland Sea indicates the area of previous pCO_2 data analysis. The inset shows the sub-transect selected for the analysis of the pCO_2 data in the Mecklenburg Bight (dashed ellipse), the sampling position for the determination of nutrient concentrations (circle) and the two stations for the analysis of the cyanobacteria abundance (stars).

Based on the second pCO₂ minimum the mid-summer NCP was determined and, using the C/N ratio of particulate organic matter (POM), facilitated the estimate of the nitrogen fixation. Furthermore, it was shown that the exposure to solar radiation is the major control for the development of the cyanobacteria bloom and that the temperature as such plays only a minor role. In contrast to the Baltic Proper, blooms of nitrogen-fixing species are not a common phenomenon in western Baltic Sea. Therefore the annual Environmental Fact Sheet of HELCOM on the “Cyanobacteria Biomass” did not consider the western Baltic Sea (Wasmund et al., 2014) and published data on cyanobacteria abundance from this area are rare.

Here we present the pCO₂ data collected during 2003–2014 in the Mecklenburg Bight located in the southwest of the Baltic Sea (Fig. 1). This region has not been included into our previous data analysis since it has specific hydrographic characteristics due to its location in the highly dynamic transition zone between the North Sea and the Baltic Proper. We are aiming at the determination of the timing, the intensity and the relationship to the nutrient availability of the spring bloom in the Mecklenburg Bight. Furthermore, the data will be analyzed for evidence of mid-summer production based on nitrogen fixation.

2. Methods

2.1. Cruise details

The route of cargo ship “Finnpartner” that was replaced by “Finnmaid” in 2007, between the Mecklenburg Bight and the Gulf of Finland is shown in Fig. 1. The measurements were stopped when the ship passed polluted waters in the vicinity of the ports of destination. When leaving the harbour area, the measurements system was first calibrated before the pCO₂ measurements started. For the study presented here, we used the mean pCO₂, temperature and salinity from the eastern part of the Mecklenburg Bight (12.0°E–12.6°E, Fig. 1, inset). The temporal resolution of the data resulted from the frequency of transits, the annual docking period of 1–2 weeks and occasional malfunctions of the measurement system. For example, in 2014 we obtained 160 pCO₂ transects across the entire Baltic Proper which corresponded to a mean temporal resolution of 2.7 days.

2.2. Analytical methods

The pCO₂ measurements were based on equilibration of air with surface water and determination of the CO₂ content in the equilibrated air by infrared detection (Licor 6262). Therefore, surface water from a depth of about 3 m is continuously pumped into a bubble-type equilibrator, while at the same time air is pumped in a closed loop through the water column in the equilibrator. The infrared spectrometer that is integrated into the air loop, is equipped with a channel for the analysis of both CO₂ and water vapour and displays the CO₂ mole fraction in dry air. Furthermore, the water temperature in the equilibrator and the pressure in the headspace of the equilibrator are measured in order to account for the temperature increase during pumping (~1 K) and to convert the CO₂ mole fraction into pressure units. The spatial

resolution of the pCO₂ data is given by the equilibration time (e-fold equilibration time ~5 min) and by the ship's speed (about 20 knots), and amounts thus to about 2 nautical miles. The estimated uncertainty of the measurements amounts to less than 5 μatm. The pCO₂ measurements were accompanied by records of the in situ temperature (SST) and salinity (S). More details about the measurement system and the procedure to calculate the in situ pCO₂ from the mole fraction in dry air are given in Koertzing et al. (1996).

For the determination of the nutrient concentrations 24 samples were taken automatically along the route of “Finnmaid” at irregular time intervals of 1–4 weeks. One sampling position was located within the Mecklenburg Bight sub-transect at 12.5°E (Fig. 1). The samples were analyzed in the home laboratory immediately after arrival of “Finnmaid” in the harbour (Helsinki). The concentrations of nitrate and phosphate were determined on the basis of the classical photometric methods (Grasshoff et al., 1983). Ammonium concentrations were measured only sporadically during the first years of our study. Since the concentrations were in general below 0.5 μmol L⁻¹, ammonium is neglected when considering the availability of nitrogen for primary production and the dissolved inorganic nitrogen (DIN) is given by the nitrate concentrations.

2.3. Calculation of the CO₂ gas exchange

The CO₂ flux by gas exchange at the sea surface was calculated according to:

$$F_{\text{CO}_2}^{\text{AS}} = k_{660} \cdot \left(\frac{Sc}{660}\right)^{-0.5} \cdot k_0 \cdot (\text{pCO}_2^{\text{atm}} - \text{pCO}_2), \quad (1)$$

with k_{660} the gas exchange transfer velocity normalized to a Schmidt number of 660, Sc the Schmidt number, k_0 the CO₂ solubility constant (function of temperature and salinity, Weiss, 1974), pCO₂ the surface water pCO₂ and pCO₂^{atm} the atmospheric CO₂ partial pressure.

The atmospheric CO₂ partial pressure, pCO₂^{atm}, was calculated from the mole fraction of CO₂ in dry air that was determined in air over the central Baltic Sea in 2005 (Schneider et al., 2014a). For the calculations water vapour saturation was assumed at the sea surface. To transfer the data to individual years before/after 2005, an annual increase of the atmospheric CO₂ of 2 ppm was taken into account (Keeling et al., 2008). The Schmidt number, Sc , that accounts mainly for the temperature dependency of the gas exchange transfer velocity, was calculated according to Wanninkhof (1992) for zero salinity. The variable k_{660} represents the gas exchange transfer velocity normalized to $Sc = 660$ that corresponds to the transfer velocity of CO₂ at 20°C and a salinity of 35. The dependency of k_{660} on wind speed (at a height of 10 m, u_{10}) was parameterized by a quadratic function (Wanninkhof et al., 2009):

$$k_{660} = 0.24 \cdot u_{10}^2. \quad (2)$$

Geostrophic wind speed data (u_{10}) for the southwest Baltic Sea were obtained from the Swedish Meteorological and Hydrological Institute (SMHI) and reduced to the wind speed at 10 m height according to Omstedt and Axell (2003). Mean u_{10} were calculated for the determination of daily fluxes, whereas the variables (Eq. (1)) with a lower temporal resolution were linearly interpolated.

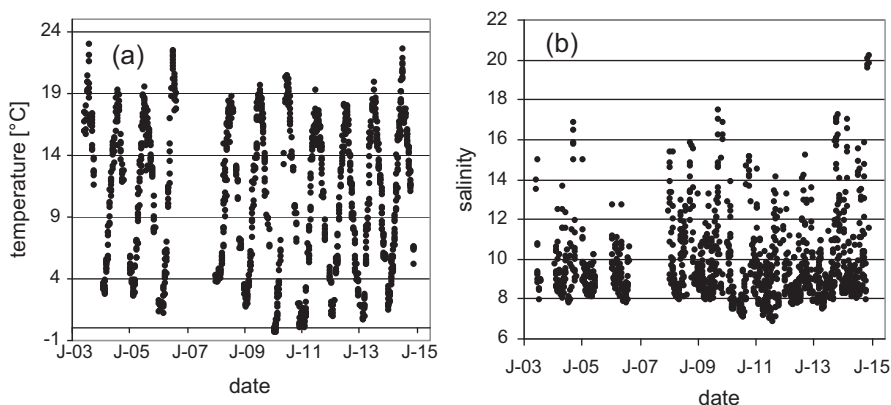


Figure 2 Time series of the (a) mean surface water temperature and (b) salinity along the transect in the Mecklenburg Bight.

2.4. Calculation of changes in total CO_2 concentrations

For the determination of the NCP on the basis of the CO_2 consumption, it is necessary to convert changes in pCO_2 to changes in the total CO_2 concentrations, C_T . This is facilitated by the fact that the abundance of calcifying plankton is negligible in the Mecklenburg Bight and that thus significant internal alkalinity (A_T) changes do not occur. But varying salinities during the individual periods for the NCP determination indicate that different water masses with different A_T were encountered. These cause changes in C_T which are not related to biological CO_2 consumption or gas exchange. Hence, it is not meaningful to calculate the in situ C_T from the in situ A_T and the pCO_2 measurements. Instead, we used the measured pCO_2 and the mean A_T for the considered time span to calculate the C_T . The C_T calculated in this way may be considered as the C_T normalized to the mean A_T and its changes, ΔC_T , are no longer affected by variations in A_T and are equivalent to the CO_2 loss by organic matter production that is partly compensated for by gas exchange.

For the determination of ΔC_T on the basis of the pCO_2 data, we used the in situ SST and salinity, and the mean A_T ($1,696 \mu\text{mol kg}^{-1}$). The latter resulted from the mean salinity (9.4) during the development of the spring bloom and the salinity–alkalinity relationship for the area south of the Gotland Sea (Schneider et al., 2010). The computations were then performed by the use of the equilibrium constants of the marine CO_2 system (Millero et al., 2006; Weiss, 1974). Since the relationship between the observed change in pCO_2 and the calculated ΔC_T is not entirely independent on A_T , the uncertainty of ΔC_T that is associated with the choice of the mean A_T , was calculated. Based on the standard deviation of A_T ($\pm 43 \mu\text{mol kg}^{-1}$) that was obtained from the variability of the salinity during the individual spring bloom periods, an uncertainty of $\pm 3\%$ was obtained for ΔC_T . When using instead the maximum difference between the mean A_T and individual A_T (about $100 \mu\text{mol kg}^{-1}$) the difference in ΔC_T amounted to $\pm 7\%$.

3. Results and discussion

3.1. Hydrography

The Mecklenburg Bight is part of the transition zone between the Baltic Sea and the North Sea. The mean depth along the

sub-transect of our data analysis is about 25 m. The Mecklenburg Bight is characterized by the outflow of low-salinity Baltic seawater and the inflow of North Sea water with a higher salinity. This leads to a salinity stratification at an average depth of about 10–15 m. Due to fast changing wind driven inflow/outflow conditions and to vertical mixing, the surface salinities show a large short-term variability and range between about 7 and 18 (Fig. 2b). In most of the years the salinity maxima occurred in autumn and winter, however, in some years high salinities were also observed during summer and only the long-term mean salinity distribution reveals a clear seasonality. The extreme salinities of about 20 observed in December 2014 were the precursor of a major inflow of high-salinity water from the North Sea that has caused the renewal of stagnant and anoxic water masses in the deep basins of the Baltic Proper (Mohrholz et al., 2015).

Surface water temperatures show a distinct seasonal cycle (Fig. 2a). Temperature maxima of about 19–23°C are observed in July/August whereas the temperature minima range between 4°C and slightly below 0°C in February/March. Sea ice formation that occurred in rare cases, was generally restricted to regions close to the coast.

3.2. Time series and seasonality of the pCO_2

The mean pCO_2 along the sub-transect in the Mecklenburg Bight is shown in Fig. 3. The data gap in 2007 was caused by the changeover of the instrumentation from “Finnpartner” to “Finnmaid”. The data show a distinct seasonality with minimum pCO_2 due to CO_2 consumption during the spring bloom. The pCO_2 maxima in autumn/winter are attributed to mixing with deeper water masses that have been in contact with the sediment surface and are enriched in CO_2 by mineralization of organic matter. Fig. 3 also indicates an increase of the seasonal pCO_2 amplitude resulting from both enhanced pCO_2 maxima and more pronounced pCO_2 minima. This points to an increased net community production during spring/summer during the last decade and consequently to an intensified organic matter mineralization at the sediment surface.

Details of the seasonal pCO_2 cycle are visible in Fig. 4a that presents the pCO_2 data from all years as a function of the Julian day. For comparison, the mean pCO_2 in the eastern Gotland Sea (Fig. 1) from the same years are shown in Fig. 4b. In order to account for the increasing atmospheric CO_2 (2 ppm yr^{-1}) that causes a corresponding shift of the surface

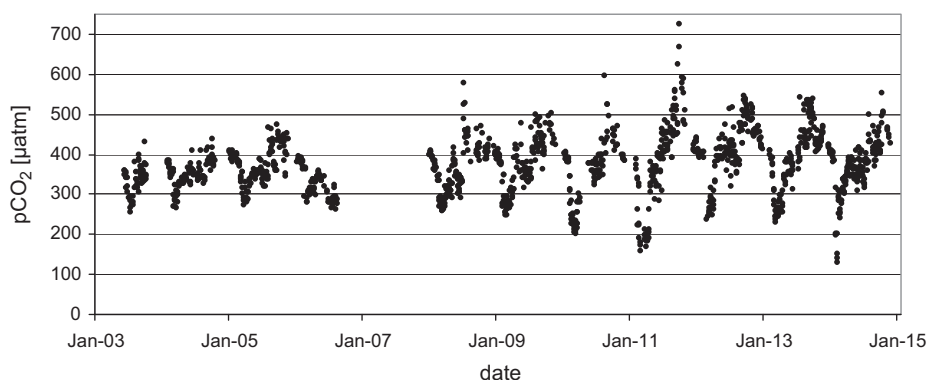


Figure 3 Time series of the mean surface water CO_2 partial pressure along the transect in the Mecklenburg Bight.

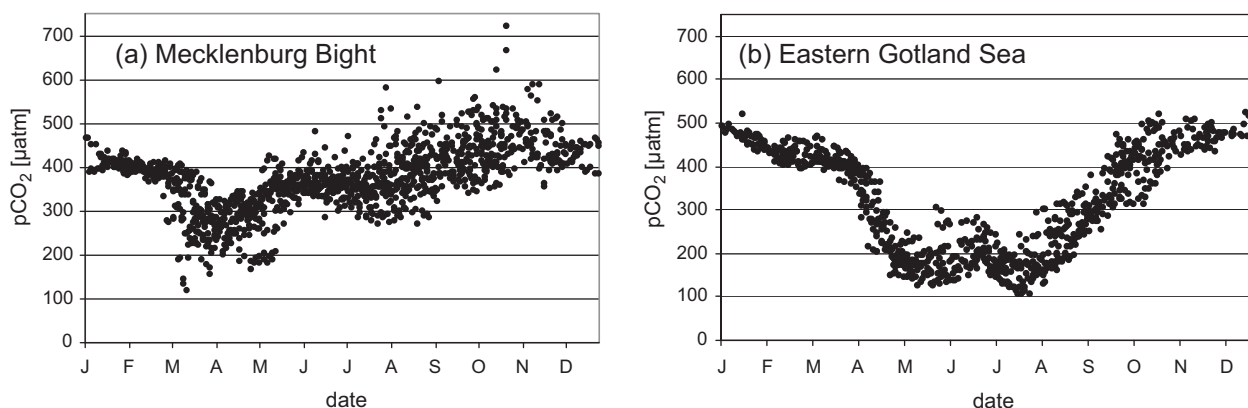


Figure 4 Seasonality of the mean surface water CO_2 partial pressure in the (a) Mecklenburg Bight and in the (b) eastern Gotland Sea. The data were collected during 2003–2014 and are normalized to 2010 by accounting for the annual increase of the atmospheric CO_2 (2 ppm).

water pCO_2 , the data were approximately adjusted to the year 2010 by adding/subtracting an annual offset of $2 \mu\text{atm}$ to the data. The seasonal pCO_2 distribution in the Gotland Sea is characterized by two pronounced minima which are observed in April/May and in July/August and which can be attributed to NCP in spring and during the nitrogen fixation in midsummer, respectively. The spring draw down of the pCO_2 occurs also in the Mecklenburg Bight, however, the minimum is less distinctive. In the Mecklenburg Bight there is only a slight hint for a pCO_2 minimum in mid-summer. Furthermore, the pCO_2 variability during late summer and autumn is much stronger in the Mecklenburg Bight than in the Gotland Sea. This is not the consequence of the interannual variability, but it is caused by the high pCO_2 variability within individual years. The latter can be explained by the low water depth that favours sporadic wind driven mixing with CO_2 -enriched bottom water that is alternating with inflow of CO_2 -depleted surface water from the Baltic Proper. During winter the pCO_2 evens out at and approaches the atmospheric level of about $400 \mu\text{atm}$ at the start of the spring bloom in February/March. This is the case in both the Mecklenburg Bight and in the Gotland Sea, and is attributed to the gradual equilibration of the surface water with the atmospheric CO_2 by gas exchange.

3.3. Characteristics of the spring bloom

The spring bloom starts as soon as the phytoplankton receives sufficient light to maintain net growth. In the Baltic Proper this is the case when vertical mixing is confined to the photic zone (about 30 m). This happens during the development of a shallow thermal surface layer that prevents plankton from circulating through dark deeper layers (Smetacek and Passow, 1990) and that increases the mean exposition of plankton to sunlight (Wasmund et al., 1998). In the shallow waters of the Mecklenburg Bight with a mean depth of about 25 m, one may therefore expect that the spring bloom starts each year at approximately the same date when the daily solar radiation has exceeded a certain threshold value. However, this conclusion contrasts with the results of our approach to identify the start of the spring bloom. We considered the first continuous decrease of the surface water pCO_2 below the atmospheric pCO_2 ($\Delta\text{pCO}_2 < 0$) that could not be explained by a decrease in temperature, as the start of the spring bloom. According to this definition the spring bloom started within a time slot of 5 weeks from February 12 to March 21. To illustrate the temporal development of the spring bloom, the ΔpCO_2 together with the SST are shown for the years 2005 and 2009 (Fig. 5a and b). In 2009 the ΔpCO_2 dropped below the

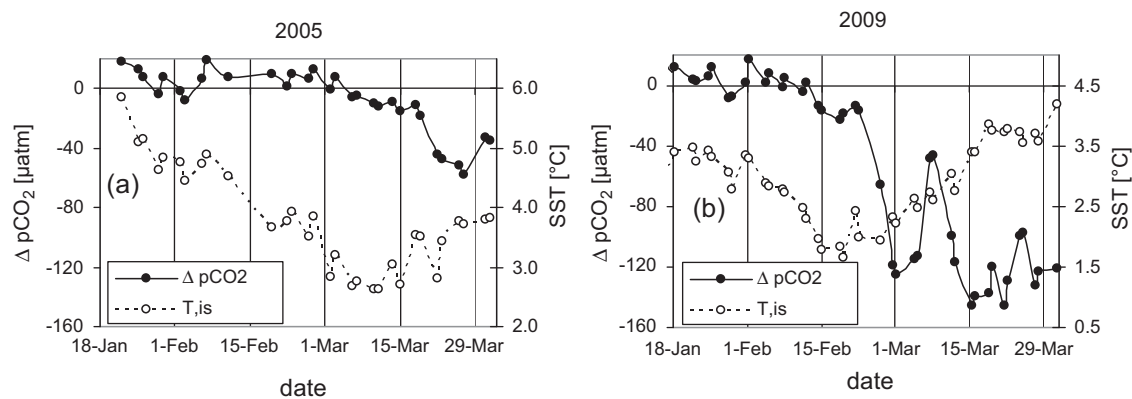


Figure 5 Two examples for the temporal development of difference between the surface water and atmospheric $p\text{CO}_2$, $\Delta p\text{CO}_2$, (full circles) and of the surface water temperature, SST, (open circles) during early spring. Continuous CO_2 undersaturation of the surface water ($\Delta p\text{CO}_2 < 0$) indicates the start of the spring bloom.

zero line on February 12 whereas in 2005 this happened much later, on March 6. The delay of the spring bloom in 2005 occurred although the temperature by mid-February was higher than at the same time in 2009 when the early spring bloom start was observed. Hence, the temperature as such does obviously not control the development of the plankton bloom. However, Fig. 5a and b indicate that the first slight $p\text{CO}_2$ decrease coincided with the minimum of the SST and that a stronger $p\text{CO}_2$ decrease followed when the SST started to increase. This shows that despite the low water depth the spring bloom is triggered by the development of a shallow thermocline as reflected by the reversal of the winter cooling towards higher SST. Fig. 5 also illustrates that the spring bloom $p\text{CO}_2$ decrease does not occur strictly in a steady way, but is superimposed by temporal fluctuations. In case of the strong temporary peak in Fig. 5b, this can be explained by wind-driven strong vertical mixing and transport of water masses to the surface that were less exposed to photosynthesis. On the other hand, during extremely calm conditions when mixing is widely inhibited, it is conceivable

that the $p\text{CO}_2$ determined in water from a depth of about 3 m differs from the value that is obtained when mixing reaches again the main thermocline.

The spring bloom is fuelled by nitrate and phosphate that accumulated in the surface water during winter. Fig. 6 shows that the NO_3^- is rapidly consumed and, with one exception, stays below $0.2 \mu\text{mol L}^{-1}$ from mid March until the end of August. This is not the case for PO_4^{3-} that in most years still existed at substantial concentrations throughout the productive period. An exception is the year 2011 (Fig. 6, green line) when extraordinarily high NO_3^- concentrations were observed and yielded a nutrient N/P ratio of 25 at the start of the spring bloom. Hence, based on the fact that the nutrient uptake by plankton occurs according to the classical N/P Redfield ratio (16), no PO_4^{3-} is left over after the consumption of NO_3^- . In contrast, one could expect an excess of NO_3^- , which, however, is not observed possibly because of enhanced nitrogen uptake by plankton. But we must also take into account the hydrographic dynamics in the Mecklenburg Bight that limits the interpretation of data from a single station.

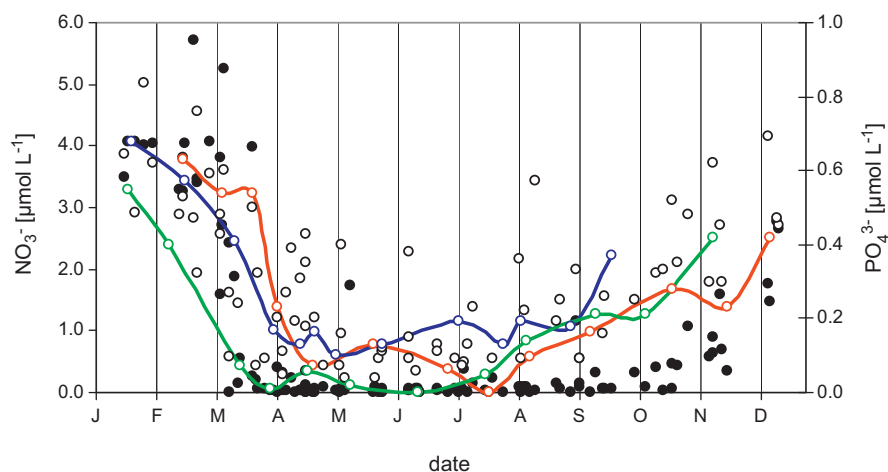


Figure 6 Seasonality of the nitrate (full circles) and phosphate (open circles) concentrations at the sampling location on the Mecklenburg Bight transect. The coloured lines represent years with different seasonal characteristics of the phosphate concentrations: (green) no phosphate excess in the winter nutrient pool; (blue) phosphate excess of the winter nutrient pool is retained throughout spring and summer; (red) phosphate excess of the winter nutrient pool decreases after the nitrate depletion in spring.

Table 1 Periods between the start of the spring bloom and the date of the nitrate depletion, consumption of nitrate (ΔNO_3) and phosphate (ΔPO_4), total CO_2 depletion (ΔC_T) and net community production (NCP) during the spring bloom in the Mecklenburg Bight. The elemental ratios C/N, C/P and N/P of particulate organic matter are calculated on the basis of ΔNO_3 , ΔPO_4 and NCP.

Time period	ΔNO_3 [$\mu\text{mol L}^{-1}$]	ΔPO_4 [$\mu\text{mol L}^{-1}$]	ΔC_T [$\mu\text{mol kg}^{-1}$]	NCP [$\mu\text{mol L}^{-1}$]	C/N	C/P	N/P
22.2.04–28.3.04	3.5	0.23	31.5	35.3	10.0	154	15
6.3.05–5.4.05			23.6	22.2			
22.2.06–21.3.06	3.4	0.26	15.3	17.4	5.2	67	13
13.2.08–24.3.08	3.4	0.16	19.3	33.1	9.7	207	21
15.2.09–1.4.09	4.2	0.40	25.6	42.8	10.2	107	11
15.2.10–14.3.10	3.8	0.29	38.5	36.3	9.5	125	13
7.2.11–30.3.11	10.4	0.39	66.0	75.0	7.2	192	27
7.3.12–3.4.12	5.4	0.40	50.5	50.1	9.3	125	14
21.3.13–3.4.13	3.7	0.31	31.6	30.4	8.4	98	12
20.2.14–9.3.14	5.8	0.37	50.6	49.6	8.6	134	16
Mean					8.7	134	16
Std. dev.					1.6	44	5

In all other years the N/P ratios of the winter nutrient pool ranged between 5 and 12 and were thus considerably below the Redfield ratio of 16. As a consequence, a PO_4 excess existed and was still observed after the complete exhaustion of NO_3 . In most years the PO_4 excess was preserved throughout the productive period as shown by the blue line in Fig. 6. However, in some years the initial PO_4 decrease continued after the NO_3 depletion (Fig. 6, red line) and was accompanied by a decrease in $p\text{CO}_2$. Similar observations were made in the central Gotland Sea and lead to the conclusion that net production had occurred despite the lack of nitrogen (Schneider et al., 2009). Here we hesitate to postulate the continuation of the net community production and to speculate about a potential nitrogen source (Eggert and Schneider, 2015) because the $p\text{CO}_2$ did not always follow the PO_4 trend and because the high variability did not allow for an unambiguous interpretation of the nutrient data. Therefore, we consider the spring bloom in the Mecklenburg Bight to be limited by the nitrogen (nitrate) availability. To quantify the NCP, we first calculated the total CO_2 decrease, ΔC_T , between the start of the spring bloom and the date when the nitrate concentrations dropped to about $0.5 \mu\text{mol L}^{-1}$ or

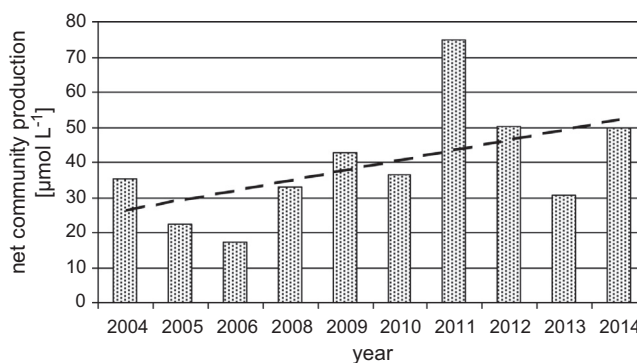


Figure 7 Net community production in the Mecklenburg Bight. The regression line corresponds to a mean increase of about 80% during 2004–2014.

below this value (Table 1). To account for the CO_2 gas exchange that partly compensates the biogenic CO_2 loss, the CO_2 flux was calculated (Eq. (1)) for the same period. Dividing the CO_2 flux by the mixing depth (20 m) yielded the effect of the gas exchange on C_T (ΔC_T^{AS}). The sum of ΔC_T and

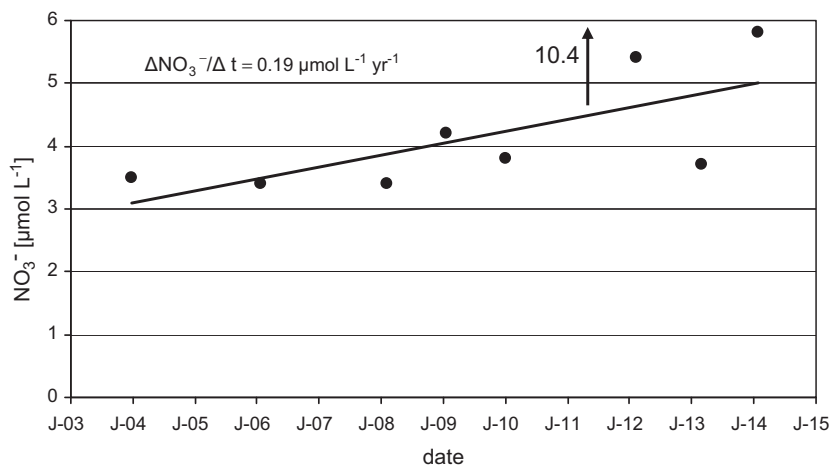


Figure 8 The nitrate concentrations in the Mecklenburg Bight at the start of the spring bloom. The regression line was calculated without the extreme nitrate concentration in 2011 ($10.4 \mu\text{mol L}^{-1}$) and corresponds to a mean increase of 63% during 2004–2014.

ΔC_T^{AS} represents the internal C_T loss that in the absence of calcium carbonate formation is equivalent to the net organic matter production. The mean contribution of the ΔC_T^{AS} term to the calculated organic matter production amounted to 35% and constitutes the major uncertainty in our estimate. The net production of particulate organic matter, termed here NCP, is obtained (Table 1, Fig. 7) by assuming that 20% of the produced organic matter contributes to the dissolved organic matter pool (Hansell and Carlson, 1998; Schneider and Kuss, 2004). A linear regression analysis indicates that the NCP increased by roughly 80% during 2004–2014 (Fig. 7). The mean NCP amounted to $40 \mu\text{mol L}^{-1}$ and corresponds to an integrated production of 0.8 mol m^{-2} when assuming a depth of the mixed layer of 20 m.

The NCP increase is also reflected in an increase of the winter nitrate concentrations (Table 1, Fig. 8). Neglecting the extremely high nitrate concentration in 2011 ($10.4 \mu\text{mol L}^{-1}$), the regression line yields a mean increase of the winter nitrate of $0.19 \mu\text{mol L}^{-1} \text{ yr}^{-1}$ and corresponds to an increase of 63% during the period 2004–2014. This is by about 25% less than the NCP increase, but we must take into account that the nutrient data were obtained at just one station and had a lower temporal resolution.

Finally, we related the NCP to the consumption of nitrate and phosphate (Table 1) during the respective time period. In the case of the nitrate, the atmospheric deposition of dissolved inorganic nitrogen (DIN = nitrate + ammonium) was taken into account. We used the deposition estimate by Bartnicki et al. (2011) and distributed the flux of $0.1 \text{ mmol m}^{-2} \text{ yr}^{-1}$ within the upper 20 m of the surface water. The nitrate and phosphate depletion in 2005 were by some reason out of phase and were therefore omitted from the analysis of the elemental ratios during the spring bloom. The mean C/N and C/P ratios (Table 1) amounted to 8.7 ± 1.6 and 134 ± 44 , respectively, and indicate a slight carbon enrichment with respect to nitrogen and phosphorus when compared with the classical C/N and C/P ratios of 6.6 and 106, respectively. The mean N/P ratio was 16 ± 5 and agreed perfectly with the Redfield N/P ratio despite the high standard deviation of the individual ratios.

3.4. Mid-summer nitrogen fixation

In contrast to the Gotland Sea, mid-summer $p\text{CO}_2$ minima did not occur regularly in the Mecklenburg Bight (Fig. 4a and b). Nonetheless, distinct $p\text{CO}_2$ minima were detected in June/July of 2006 and 2008 (Fig. 9a and b, shadowed area). Since the decrease in $p\text{CO}_2$ was not accompanied by a lowering of the salinity, we could exclude that advection of low- CO_2 water from the Baltic Proper was the cause of the $p\text{CO}_2$ decrease, but rather on-site NCP in this area of the Mecklenburg Bight. The onset of the mid-summer production becomes also evident by the plot of the $p\text{CO}_2$ versus SST (Fig. 10). After the spring bloom minimum, the $p\text{CO}_2$ increased with rising SST because the temperature effect on the $p\text{CO}_2$ prevailed over any NCP. However, by about May 28 the $p\text{CO}_2$ started to decrease despite the continuation of the SST increase and indicates the start of a NCP period.

The mid-summer NCP were calculated in the same manner than the previous calculations for the spring NCP bloom except for the choice of the mixed layer depth. Here we

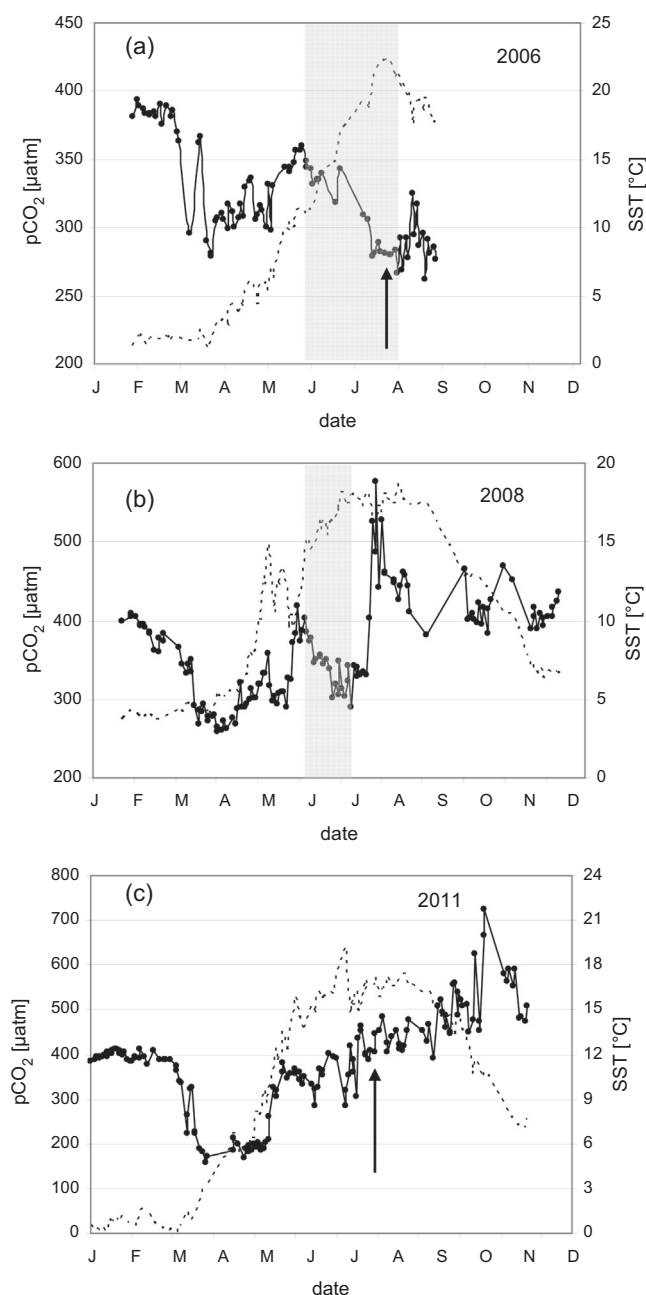


Figure 9 The seasonality of the $p\text{CO}_2$ and sea surface temperature in (a and b) two years with a distinct mid-summer minimum of the $p\text{CO}_2$ (shadowed area) and (c) a year without a prolonged mid-summer minimum.

used a value of only $z_{\text{mix}} = 10 \text{ m}$ which is consistent with the vertical temperature distribution at monitoring stations in the Mecklenburg Bight (IOW, unpublished data) and which is more plausible in view of the rapid SST increase during the considered periods. For the two selected periods from May 28 to August 5 (2006) and from June 3 to June 29 (2008) the NCP amounted $60 \mu\text{mol L}^{-1}$ and $45 \mu\text{mol L}^{-1}$, respectively. Since the nitrate concentrations were virtually zero during this time of the year, we concluded that nitrogen fixation provided nitrogen for the NCP. To quantify the nitrogen demand, the NCP was divided by the C/N ratio (8.4) of

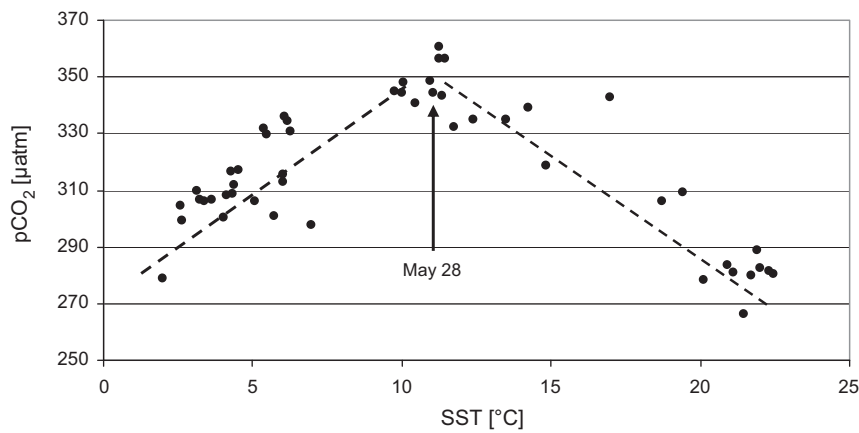


Figure 10 The $p\text{CO}_2$ as a function of the sea surface temperature during the transition from late spring to summer 2006.

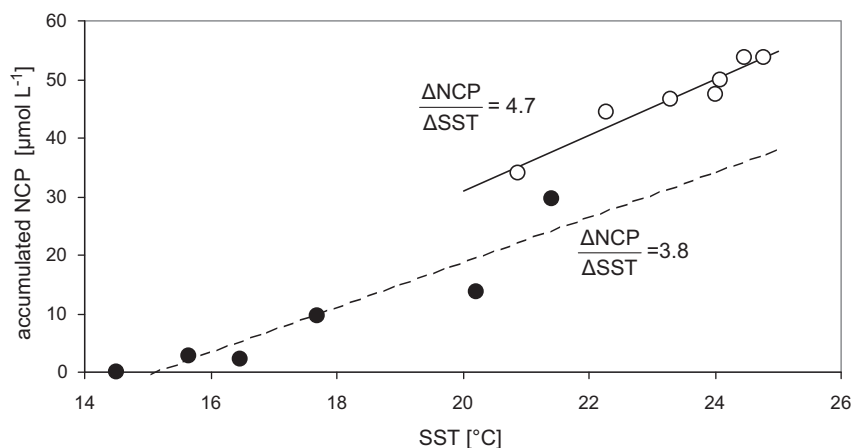


Figure 11 Relationship between the accumulated NCP and temperature during two phases of continuous temperature increase in 2006.

POM that was observed during periods of nitrogen fixation in the central Baltic Sea (Schneider et al., 2003). Taking into account the atmospheric deposition of DIN ($0.26 \mu\text{mol L}^{-1}$ and $0.69 \mu\text{mol L}^{-1}$), the nitrogen fixation amounted to $6.4 \mu\text{mol-N L}^{-1}$ and $5.1 \mu\text{mol-N L}^{-1}$ for 2006 and 2008, respectively. Based on a mixed layer depth of 10 m, these estimates correspond to depth-integrated values of 64 mmol-N m^{-2} and 51 mmol-N m^{-2} and are by a factor of about 2 below the mean N_2 fixation ($138 \text{ mmol-N m}^{-2}$) that was obtained from $p\text{CO}_2$ records in the eastern Gotland Sea by Schneider et al. (2014a).

The Gotland Sea study by Schneider et al. (2014a) revealed clear relationships between the accumulated NCP and temperature during periods of nitrogen fixation in different years. This has led to the conclusion that the ratio between solar radiation and mixed layer depth – hence the exposure of plankton particles to sunlight – controls both the temperature and the nitrogen fixation. The data from the Mecklenburg Bight showed two longer periods with continuously rising temperatures during the suspected nitrogen fixation period in 2006. These were used to plot the accumulated NCP as a function of SST (Fig. 11). Reasonable linear relationships were found for both phases with slopes that amounted to 4.7 and $3.8 \text{ mmol-C L}^{-1} \text{ K}^{-1}$ and that are by a factor of 3–4 lower than during nitrogen fixation in the central Gotland Sea ($11\text{--}16 \text{ mmol L}^{-1} \text{ K}^{-1}$).

The pronounced mid-summer NCP in 2006 that was attributed to nitrogen fixation, is consistent with investigations of the composition of the plankton community. These were performed within the IOW monitoring programme at two stations (12 and 46) in the Mecklenburg Bight (Fig. 1). The results of the cyanobacteria counting for the years 2004–2014 (Table 2) show the second largest cyanobacteria abundance by the end of July in 2006 when the $p\text{CO}_2$ minimum was observed. Furthermore, 2006 was the only year in a time series of satellite images that showed distinct summer blooms in the Mecklenburg Bight (Öberg, 2013). In that year the blooms were so severe that some beaches in northwestern Mecklenburg had to be closed in the beginning of August. The second significant mid-summer NCP derived from the $p\text{CO}_2$ data occurred in 2008, which, however was not reflected in an outstanding cyanobacteria abundance at the two stations in the Mecklenburg Bight. Vice versa, the highest cyanobacteria biomass detected in August 2011 was not reflected in a draw down of the $p\text{CO}_2$ (Fig. 9c). However, previous to the date of the biological observations the $p\text{CO}_2$ shows short-term decreases in July during which the $p\text{CO}_2$ dropped to about $300 \mu\text{atm}$ (unfortunately this is somewhat masked in Fig. 9c because of the wide $p\text{CO}_2$ range in 2011). These low $p\text{CO}_2$ coincided with the increase of SST and may reflect nitrogen

Table 2 Cyanobacteria biomass during mid-summer at two stations in the Mecklenburg Bight (bold letters indicate agreement between high biomass and high nitrogen fixation estimate).

Year	Station 12		Station 46	
	Date	Biomass [mg m^{-3}]	Date	Biomass [mg m^{-3}]
2004	14.07.2004	87.2	22.07.2004	42.0
2005	20.07.2005	132.0	21.07.2005	45.6
2006	27.07.2006	235.0	27.07.2006	168.0
2007	27.07.2007	50.1	27.07.2007	67.6
2008	01.07.2008	76.6	30.07.2008	38.2
2009	25.07.2009	54.0	25.07.2009	57.7
2010	25.07.2010	116.6	25.07.2010	104.1
2011	04.08.2011	252.2	14.08.2011	175.6
2012	04.08.2012	41.1	26.07.2012	32.6
2013	08.08.2013	62.9	08.08.2013	28.1

fixation events which was still detectable as high biomass in August.

4. Summary and conclusions

Despite the strong hydrographic dynamics in the transition area between the North Sea and the Baltic Sea, measurements of the surface water pCO_2 are a useful tool to study basic biogeochemical processes in the Mecklenburg Bight. The start of the spring bloom in different years could unambiguously and precisely be determined by the drop of the pCO_2 below the atmospheric level. It was shown that the temperature as such does not control the onset of the spring bloom, but that also in the Mecklenburg Bight with a mean water depth of only about 25 m, the development of a shallow surface layer is a prerequisite for efficient photosynthesis.

According to the increasing seasonal pCO_2 amplitude, the pCO_2 based calculations of the net community production shows a trend that amounts to an increase of about 80% during 2004–2014. Future measurements will show whether this is a long-term development or a result of decadal variability. We concede that the calculation of the NCP may be associated with systematic biases. These are partly due to the gas exchange calculations which are mainly affected by uncertainties in the parameterization of the transfer velocity, k_{660} , with wind speed (Eq. (2)). However, even if assuming an extreme error in k_{660} by 50%, the impact on the calculations of the NCP is on average only 17%, because the gas exchange term contributes only 35% to the calculated NCP. Furthermore, the use of the 20% DOC contribution to the organic matter production is prone to an error which, however, is difficult to quantify. On the other hand, the elemental C/N and C/P ratios of particulate organic matter which are based on the calculation of the NCP, are widely consistent with the standard Redfield stoichiometry and indicate that our NCP estimate was not unreasonable.

Decreasing CO_2 partial pressure during mid-summer in particular years indicated NCP fuelled by nitrogen fixation since DIN concentrations were virtually zero and since the atmospheric DIN deposition could not satisfy the nitrogen demand of DIN. This was confirmed by biological investigations which showed a cyanobacteria biomass peak

in a year (2006) when the most extended pCO_2 mid-summer was found. However, this coincidence was not observed in another year with high cyanobacteria biomass. Based on the calculated NCP and a C/N ratio of particulate organic matter (8.4), the nitrogen fixation activity was estimated for two years, 2006 and 2008, which revealed unambiguously a mid-summer pCO_2 minimum. We obtained values of 64 mmol-N m^{-2} and 51 mmol-N m^{-2} , respectively, which are considerably below the mean nitrogen fixation in the central Baltic Sea that according to the most recent pCO_2 -based estimates amounts $138 \text{ mmol-N m}^{-2}$ (Schneider et al., 2014b). Since furthermore the nitrogen fixation determined for 2006 and 2008 do not represent a mean, but are exceptional events observed during 2004–2014, we conclude that nitrogen fixation in the Mecklenburg Bight and possibly in the entire transition area to the North Sea is of minor importance for the Baltic Sea nitrogen budget.

The increased nitrogen fixation activity in the central Baltic Sea is also reflected in the relationship between the accumulated mid-summer NCP and temperature. The latter can be interpreted as the dependency of nitrogen fixation on the exposure of plankton to solar radiation that can be approximated by the increase in temperature. The average $\Delta\text{NCP}/\Delta T$ for the eastern Gotland Sea calculated from six nitrogen fixation events amounted to $12.5 \pm 1.8 \mu\text{mol L}^{-1} \text{K}^{-1}$, whereas the mean for the Mecklenburg Bight was 4.3 (3.8 and 4.7) $\mu\text{mol L}^{-1} \text{K}^{-1}$. Hence, the nitrogen fixation efficiency (reflected in the NCP) in the eastern Gotland Sea was by a factor of three larger than in the Mecklenburg Bight. This is possibly due to the higher salinity in the Mecklenburg Bight that may slowdown nitrogen fixation (Stal et al., 2003).

Acknowledgements

This study is based on measurements on cargo ships “Finnpartner” and “Finnmaid” and were performed in a cooperation between the Leibniz Institute for Baltic Sea Research (IOW) in Warnemünde and the Algaline Project of Finnish Environment Institute (SYKE) in Helsinki. We appreciate very much the generous support of our research by the Finlines Shipping Company and thank especially the engine staff for their cooperation.

References

- Bartnicki, J., Semeena, V., Fagerli, H., 2011. Atmospheric deposition of nitrogen to the Baltic Sea in the period 1995–2006. *Atmos. Chem. Phys.* 11, 10057–10069.
- Eggert, A., Schneider, B., 2015. A nitrogen source in spring in the surface mixed-layer of the Baltic Sea: evidence from total nitrogen and total phosphorus data. *J. Mar. Syst.* 148, 39–47.
- Grasshoff, K., Ehrhardt, M., Kremling, K., 1983. *Methods of Seawater Analysis*, 2nd ed. Verlag Chemie, Weinheim, Germany.
- Hansell, D.A., Carlson, C.A., 1998. Net community production of dissolved organic carbon. *Global Biogeochem. Cycles* 12 (3), 443–453.
- Keeling, R.F., Piper, S.C., Bollenbacher, A.F., Walker, J.S., 2008. Atmospheric CO₂ records from sites in the SIO air sampling network. In: *Trends: A Compendium of Data on Global Change. Carbon Dioxide Information Analysis Center, Oak Ridge National Laboratory, U.S. Department of Energy, Oak Ridge, TN, U.S.A.*
- Koertzinger, A., Thomas, H., Schneider, B., Gronau, N., Mintrop, L., Duinker, J.C., 1996. At-sea intercomparison of two newly designed underway pCO₂ systems – encouraging results. *Mar. Chem.* 52, 133–145.
- Millero, F.J., Graham, T.B., Huang, F., Bustos-Serrano, H., Pierrot, D., 2006. Dissociation constants of carbonic acid in seawater as a function of salinity and temperature. *Mar. Chem.* 100 (1–2), 80–94.
- Mohrholz, V., Naumann, M., Nausch, G., Krüger, S., Gräwe, U., 2015. Fresh oxygen for the Baltic Sea – an exceptional saline inflow after a decade of stagnation. *J. Mar. Syst.* 148, 152–166.
- Öberg, J., 2013. Cyanobacterial blooms in the Baltic Sea in 2013. HELCOM Baltic Sea Environment Fact Sheets 2013, <http://helcom.fi/baltic-sea-trends/environment-fact-sheets/eutrophication/cyanobacterial-blooms-in-the-baltic-sea/>.
- Omstedt, A., Axell, L.B., 2003. Modeling the variations of salinity and temperature in the large Gulfs of the Baltic Sea. *Cont. Shelf Res.* 23, 265–294.
- Schneider, B., Gültzow, W., Sadkowiak, B., Rehder, G., 2014a. Detecting sinks and sources of CO₂ and CH₄ by ferrybox-based measurements in the Baltic Sea: three case studies. *J. Mar. Syst.* 140, 13–25.
- Schneider, B., Gustafsson, E., Sadkowiak, B., 2014b. Control of the mid-summer net community production and nitrogen fixation in the central Baltic Sea: an approach based on pCO₂ measurements on a cargo ship. *J. Mar. Syst.* 136, 1–9.
- Schneider, B., Kaitala, S., Maunula, P., 2006. Identification and quantification of plankton bloom events in the Baltic Sea by continuous pCO₂ and chlorophyll *a* measurements. *J. Mar. Syst.* 59, 238–248.
- Schneider, B., Kaitala, S., Raateoja, M., Sadkowiak, B., 2009. A nitrogen fixation estimate for the Baltic Sea based on continuous pCO₂ measurements on a cargo ship and total nitrogen data. *Cont. Shelf Res.* 29, 1535–1540.
- Schneider, B., Kuss, J., 2004. Past and present productivity of the Baltic Sea as inferred from pCO₂ data. *Cont. Shelf Res.* 24, 1611–1622.
- Schneider, B., Nausch, G., Nagel, K., Wasmund, N., 2003. The surface water CO₂ budget for the Baltic Proper: a new way to determine nitrogen fixation. *J. Mar. Syst.* 42, 53–64.
- Schneider, B., Nausch, G., Pohl, C., 2010. Mineralization of organic matter and nitrogen transformations in the Gotland Sea deep water. *Mar. Chem.* 119, 153–161.
- Smetacek, V., Passow, U., 1990. Spring bloom initiation and Sverdrup's critical depth model. *Limnol. Oceanogr.* 35, 228–234.
- Stal, L., Albertano, P., Bergman, B., von Bröckel, K., Gallon, J.R., Hayes, P.K., Sivonen, K., Walsby, A.E., 2003. BASIC: Baltic Sea cyanobacteria. An investigation of the structure and dynamics of water blooms of cyanobacteria in the Baltic Sea – response to a changing environment. *Cont. Shelf Res.* 23, 1695–1714.
- Stigebrandt, A., 1991. Computation of oxygen fluxes through the sea surface and the net production of organic matter with application to the Baltic and adjacent seas. *Limnol. Oceanogr.* 36, 444–454.
- Wanninkhof, R., 1992. Relationship between wind speed and gas exchange over the ocean. *J. Geophys. Res.* 97, 7373–7382.
- Wanninkhof, R., Asher, W.E., Ho, D.T., Sweeney, C., McGillis, W.R., 2009. Advances in quantifying air-sea gas exchange and environmental forcing. *Annu. Rev. Mar. Sci.* 1 (1), 213–244.
- Wasmund, N., Busch, S., Gromisz, S., Högländer, H., Jaanus, A., Johansen, M., Jurgensone, I., Karlsson, C., Kownacka, J., Kraśniewski, W., Lehtinen, S., Olenina, I., 2014. Cyanobacteria biomass. HELCOM Baltic Sea Environment Fact Sheet 2014, <http://www.helcom.fi/baltic-sea-trends/environment-fact-sheets/eutrophication/cyanobacteria-biomass/>.
- Wasmund, N., Nausch, G., Matthäus, W., 1998. Phytoplankton spring blooms in the southern Baltic Sea – spatio-temporal development and long-term trends. *J. Plankton Res.* 20, 1099–1117.
- Weiss, R.F., 1974. Carbon dioxide in water and seawater: the solubility of a non-ideal gas. *Mar. Chem.* 2, 203–215.